INVESTIGATION OF THE EFFECTIVENESS OF EXCITATION AND FACTS-BASED CONTROLLERS ON POWER SYSTEM STABILITY ENHANCEMENT

M. A. Abido[1], Y. L. Abdel-Magid[2]

1: Assistant Professor, Electrical Engineering Dept., King Fahd Univ. of Petroleum and Minerals
2: Professor, Electrical Engineering Dept., King Fahd Univ. of Petroleum and Minerals

E-mail: mabido@kfupm.edu.sa

ABSTRACT

Power system stability enhancement via a power system stabilizer (PSS) and FACTS-based stabilizers is thoroughly investigated in this paper. The design problem of PSS and different FACTS controllers is formulated as an optimization problem. An eigenvalue-based objective function to increase the system damping and improve the system response is proposed. Then, a real-coded genetic algorithm (RCGA) is employed to search for optimal controller parameters. In addition, this study presents a singular value decomposition (SVD) based approach to assess and measure the controllability of the poorly damped electromechanical modes by different inputs. The damping characteristics of the proposed schemes are also evaluated in terms of the damping torque coefficient with different loading conditions for better understanding of the coordination problem requirements. The proposed stabilizers are tested on a weakly connected power system with different loading conditions. The nonlinear simulation results and eigenvalue analysis show the effectiveness and robustness of the proposed control schemes over a wide range of loading conditions.

Keywords: *Power system stability, FACTS devices, and genetic algorithms*

الملخص

يقدم هذا البحث دراسة مستفيضة لتعزيز اتزان نظم القوى الكهربية من خلال مثبتات نظم القوى والمثبتات المبنية على أساس نظم نقل التيار المتردد المرنة حيث تم صياغة مشكلة تصميم هذه المثبتات فى صورة مشكلة أمثلة. ولقد تم اقتراح دالة هدف تعتمد على قيم النظام المنفردة وذلك لتحسين أداء النظام. ولقد تم تطبيق الخوارزميات الجينية ذاتالتشفير الحقيقى للحصول على التصميم الأمثل لهذه المثبتات. كذلك يقدم هذا البحث أسلوبا جديدا يعتمد على تحليل القيمة المنفردة وذلك لتقدير وقياس مدى قدرة اشارات المدخل للمثبتات المختلفة على التحكم فى الأنماط الكهروميكانيكية ذات التخميد الضعيف. وقد تم أيضا فى هذا البحث تقييم خصائص التخميد للمثبتات المقترحة باستخدام قياس معامل عزم التخميد فى ظروف التشغيل المختلفة وذلك لفهم أوضح لمتطلبات التنسيق بين هذه المثبتات. ولقد تم تطبيق المثبتات المقترحة على نظام قوى ضعيف تحت التشغيل المختلفة. ولقد أثبتت نتائج التمثيل وتحليلات القيم المنفردة فعالية الأساليب المقترحة على نطاق واسع من ظروف التشغيل المختلفة.

1. INTRODUCTION

Since 1960s, low frequency oscillations have been observed when large power systems are interconnected by relatively weak tie lines. These oscillations may sustain and grow to cause system separation if no adequate damping is available [Yu, 1983, Sauer and Pai, 1998].

Although PSSs provide supplementary feedback stabilizing signals, they suffer a drawback of being liable to cause great variations in the voltage profile and they may even result in leading power factor operation under severe disturbances. The recent advances in power electronics have led to the development of the flexible alternating current transmission systems (FACTS). Generally, a potential motivation for the accelerated use of FACTS devices is the deregulation environment in contemporary utility business. Along with primary function of the FACTS devices, the real power flow can be regulated to mitigate the low frequency oscillations and enhance power system stability. This suggests that FACTS will find new applications as electric utilities merge and as the sale of bulk power between distant and ill-interconnected partners become more wide spread.

Recently, several FACTS devices have been implemented and installed in practical power systems such as static VAR compensator (SVC) [Hammad, 1986, Padiyar and Varma, 1991], thyristor controlled series capacitor (TCSC) [Chen et al, 1995, Chang and Chow, 1997], and thyristor controlled phase shifter (TCPS) [Edris, 1991, Jiang et al, 1997]. In the literature, a little work has been done on the coordination problem investigation of excitation and FACTS-based stabilizers. Mahran et al [Mahran et al, 1992] presented a coordinated PSS and SVC control for a synchronous generator. However, the proposed approach uses recursive least squares identification which reduces its effectiveness for on-line applications. Optimum feedback strategies for both SVC and exciter controls has been presented [Rahim and Nassimi, 1996]. However, the proposed controller requires some or all states to be measurable or estimated. Moreover, it leads to a centralized controller for multimachine power systems, which reduces it applicability and reliability. A comprehensive analysis of damping of power system electromechanical oscillations using TCSC, TCPS, and SVC was presented [Noorozian and Anderson, 1994] where the impact of transmission line loading and load characteristics on the damping effect of these devices have been discussed. A coordinated fuzzy logic-based scheme for PSS and switched series capacitor modules to enhance overall power system stability was presented [Hiyama et al, 1995]. The results were promising in the sense that the power system stability region can be greatly extended. The damping torque contributed by SVC, TCSC, and TCPS has been discussed where several important points have been analyzed and confirmed through simulations [Wang and Swift, 1998]. However, all controllers were assumed proportional and no efforts have been done towards the controller design. On the other hand, it is necessary to measure the electromechanical mode controllability in order to assess the effectiveness of different controllers and form a clear idea about the coordination problem requirements.

Top

In this study, PSS and FACTS-based stabilizers are considered to enhance the damping of low frequency modes. The design problem is transformed into an optimization problem where the real-coded genetic algorithm (RCGA) will be applied to search for the optimal settings of stabilizer parameters. The effectiveness of the proposed stabilizers in enhancing the power system transient stability over a wide range of loading condition is examined. A controllability measure based on singular value decomposition (SVD) is introduced to identify the most effective stabilizer. In addition, the damping torque coefficient is evaluated with the proposed stabilizers for better understanding of coordination problem requirements. For completeness, the eigenvalue analysis and nonlinear simulation results are carried out to demonstrate the effectiveness of the proposed stabilizers to enhance system damping.

2. POWER SYSTEM MODEL

2.1. Generator

In this study, a single machine infinite bus system as shown in Fig. 1 is considered. The generator is equipped with PSS and the system has TCSC, TCPS, and SVC as shown in Fig. 1. The line impedance is $Z = R + jX$ and the generator has a local load of admittance $Y_L = g + jb$. The generator is represented by the third-order model comprising of the electromechanical swing equation and the generator internal voltage equation. The swing equation is divided into the following equations

$$\dot{\delta} = \omega_b(\omega - 1) \tag{1}$$

$$\dot{\omega} = (P_m - P_e - D(\omega - 1))/M \tag{2}$$

where, P_m and P_e are the input and output powers of the generator respectively; M and D are the inertia constant and damping coefficient respectively; δ and ω are the rotor angle and speed respectively; ω_b is the synchronous speed. The output power of the generator can be expressed in terms of the d-axis and q-axis components of the armature current, i, and terminal voltage, v, as

$$P_e = v_d i_d + v_q i_q \tag{3}$$

The internal voltage, $E_q^{'}$, equation is

$$\dot{E}_q^{'} = (E_{fd} - (x_d - x_d^{'})i_d - E_q^{'})/T_{do}^{'} \tag{4}$$

Here, E_{fd} is the field voltage; $T_{do}^{'}$ is the open circuit field time constant; x_d and $x_d^{'}$ are d-axis reactance and d-axis transient reactance of the generator respectively.

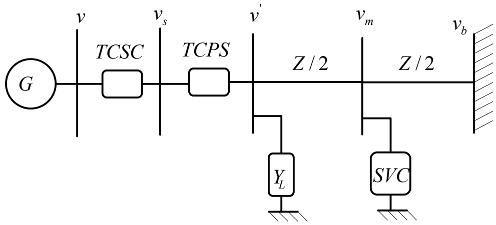

Fig. 1: Single machine infinite bus system

2.2. Exciter and PSS

The IEEE Type-ST1 excitation system shown in Fig. 2 is considered. It can be described as

$$\dot{E}_{fd} = (K_A(V_{ref} - v + u_{PSS}) - E_{fd}) / T_A \quad (5)$$

where, K_A and T_A are the gain and time constant of the excitation system respectively; V_{ref} is the reference voltage. As shown in Fig. 2, a conventional lead-lag PSS is installed in the feedback loop to generate a stabilizing signal u_{PSS}. In (5), the terminal voltage v can be expressed as

$$v = (v_d^2 + v_q^2)^{1/2} \quad (6)$$

$$v_d = x_q i_q \quad (7)$$

$$v_q = E_q^{'} - x_d^{'} i_d \quad (8)$$

where x_q is the *q*-axis reactance of the generator.

2.3. FACTS-Based Stabilizers

Fig. 3 illustrates the block diagram of an SVC with a lead-lag compensator. The susceptance of the SVC, B, can be expressed as

$$\dot{B} = (K_s(B_{ref} - u_{SVC}) - B) / T_s \quad (9)$$

where, B_{ref} is the reference susceptance of SVC; K_s and T_s are the gain and time constant of the SVC. As shown in Fig. 3, a conventional lead-lag controller is installed in the feedback loop to generate the SVC stabilizing signal u_{SVC}. The same controller structure used in Fig. 3 is applied for TCSC and TCPS by replacing SVC susceptance B by TCSC reactance X and TCPS angle Φ respectively. Similar expressions for X and Φ can be expressed as follows: -

$$\dot{X} = (K_s(X_{ref} - u_{TCSC}) - X)/T_s \tag{10}$$

$$\dot{\Phi} = (K_s(\Phi_{ref} - u_{TCPS}) - \Phi)/T_s \tag{11}$$

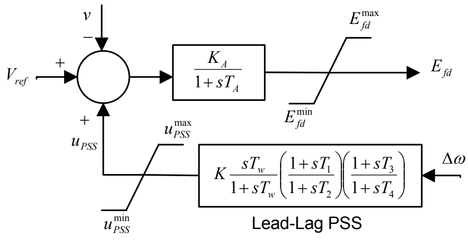

Fig. 2: IEEE Type-ST1 excitation system with PSS

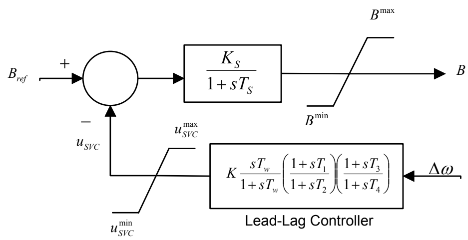

Fig. 3: SVC with lead-lag controller

2.4. Linearized Model

In the design of electromechanical mode damping controllers, the linearized incremental model around a nominal operating point is usually employed. Linearizing the expressions of i_d and i_q and substituting into the linear form of (1)-(11) yield the following linearized power system model

$$\frac{d}{dt}\begin{bmatrix}\Delta\delta \\ \Delta\omega \\ \Delta E_q' \\ \Delta E_{fd}\end{bmatrix} = \begin{bmatrix} 0 & 377 & 0 & 0 \\ -\frac{K_1}{M} & -\frac{D}{M} & -\frac{K_2}{M} & 0 \\ -\frac{K_4}{T_{do}'} & 0 & -\frac{K_3}{T_{do}'} & \frac{1}{T_{do}'} \\ -\frac{K_A K_5}{T_A} & 0 & -\frac{K_A K_6}{T_A} & -\frac{1}{T_A}\end{bmatrix}\begin{bmatrix}\Delta\delta \\ \Delta\omega \\ \Delta E_q' \\ \Delta E_{fd}\end{bmatrix} + \begin{bmatrix} 0 & 0 & 0 & 0 \\ 0 & -\frac{K_{pB}}{M} & -\frac{K_{pX}}{M} & -\frac{K_{p\Phi}}{M} \\ 0 & -\frac{K_{qB}}{T_{do}'} & -\frac{K_{qX}}{T_{do}'} & -\frac{K_{q\Phi}}{T_{do}'} \\ \frac{K_A}{T_A} & -\frac{K_A K_{vB}}{T_A} & -\frac{K_A K_{vX}}{T_A} & -\frac{K_A K_{v\Phi}}{T_A}\end{bmatrix}\begin{bmatrix}u_{PSS} \\ \Delta B \\ \Delta X \\ \Delta\Phi\end{bmatrix} \tag{12}$$

In short;

$$\dot{X} = AX + HU \tag{13}$$

Here, the state vector X is $[\Delta\delta, \Delta\omega, \Delta E_q', \Delta E_{fd}]^T$ and the control vector U is $[u_{PSS}, \Delta B, \Delta X, \Delta\Phi]^T$. The block diagram of the linearized power system model is depicted as shown in Fig. 4 where K_1-K_6, K_p, K_q, and K_v are linearization constants defined as

$$\begin{aligned} &K_1 = \partial P_e/\partial\delta,\ K_2 = \partial P_e/\partial E_q',\ K_p = \partial P_e/\partial F \\ &K_4 = \partial E_q/\partial\delta,\ K_3 = \partial E_q/\partial E_q',\ K_q = \partial E_q/\partial F \\ &K_5 = \partial v/\partial\delta,\ K_6 = \partial v/\partial E_q',\ K_v = \partial v/\partial F \end{aligned} \tag{14}$$

Top

where F is B, X, or Φ.

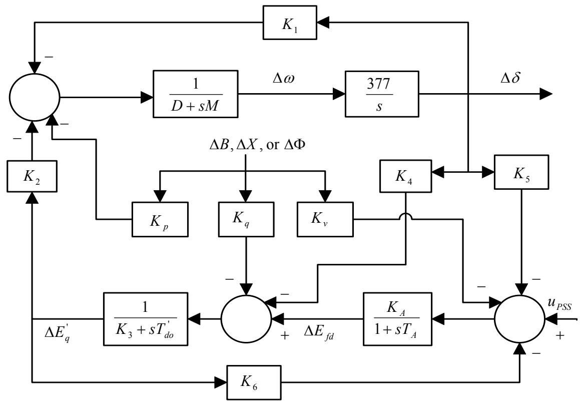

Fig. 4: Block diagram of the linearized model

3. THE PROPOSED APPROACH

3.1. Electromechanical Mode Identification

The state equation of the linearized model given in (13) is used to determine the eigenvalues of matrix A. Out of these eigenvalues, there is a mode of oscillations related to machine inertia. For the stabilizers to be effective, it is extremely important to identify the eigenvalue associated with the electromechanical mode. In this study, the participation factors method [Hsu and Chen, 1987] is used.

3.2. Controllability Measure

To measure the controllability of the electromechanical mode by a given input, the singular value decomposition (SVD) is employed in this study. Mathematically, if G is an $m \times n$ complex matrix then there exist unitary matrices W and V with dimensions of $m \times m$ and $n \times n$ respectively such that G can be written as

$$G = W \Sigma V^H \quad (15)$$

where

$$\Sigma = \begin{bmatrix} \Sigma_1 & 0 \\ 0 & 0 \end{bmatrix}, \quad \begin{array}{l} \Sigma_1 = diag(\sigma_1, \ldots\ldots, \sigma_r) \\ \text{with } \sigma_1 \geq \ldots \geq \sigma_r \geq 0 \end{array} \quad (16)$$

where $r = min\{m,n\}$ and $\sigma_1, \ldots, \sigma_r$ are the singular values of G.

The minimum singular value σ_r represents the distance of the matrix G from the all matrices with a rank of r–1. This property can be utilized to quantify modal controllability [Hamdan, 1999]. In this study, the matrix H in (13) can be written as $H = [h_1,h_2,h_3,h_4]$ where h_i is the column of matrix H corresponding to the i-th input. The minimum singular value of the matrix $[\lambda I - Ah_i]$ indicates the capability of the i-th input to control the mode associated with the eigenvalue λ. As a matter of fact, the higher the minimum singular value, the higher the controllability of this mode by the input considered. Having been identified, the controllability of the electromechanical mode can be examined with all inputs in order to identify the most effective one to control that mode.

3.3. Stabilizer Design

A widely used conventional lead-lag structure for both excitation and FACTS-based stabilizers, shown in Figs. 2 and 3, is considered. In this structure, the washout time constant T_w and the time constants T_2 and T_4 are usually prespecified. The controller gain K and time constants T_1 and T_3 are to be determined. In this study, the input signal of all proposed controllers is the speed deviation $\Delta\omega$.

In the stabilizer design process, it is aimed to maximize the damping ratio of the poorly damped electromechanical mode eigenvalues. Therefore, the following eigenvalue-based objective function J is used.

$$J = min\{\zeta: \zeta \in \zeta\text{s of electromechanical modes}\} \qquad (17)$$

where ζ is the damping ratio of the electromechanical mode eigenvalue. In the optimization process, it is aimed to *Maximize J* while satisfying the problem constraints that are the optimized parameter bounds. Therefore, the design problem can be formulated as the following optimization problem.

$$Maximize\ J \qquad (18)$$

Subject to

$$K^{\min} \le K \le K^{\max} \qquad (19)$$

$$T_1^{\min} \le T_1 \le T_1^{\max} \qquad (20)$$

$$T_3^{\min} \le T_3 \le T_3^{\max} \qquad (21)$$

The proposed approach employs RCGA to solve this optimization problem and search for optimal or near optimal set of the optimized parameters.

Top

3.4. Damping Torque Coefficient Calculation

To assess the effectiveness of the proposed stabilizers, the damping torque coefficient is evaluated and analyzed. The torque can be decomposed into synchronizing and damping components as follows

$$\Delta T_e(t) = K_{syn}\,\Delta\delta(t) + K_d\,\Delta\omega(t) \quad (22)$$

where K_{syn} and K_d are the synchronizing and damping torque coefficients respectively. It is worth mentioning that K_d is a damping measure to the electromechanical mode of oscillations [Fialat et al, 1996].

In order to calculate K_{syn} and K_d, the error between the actual torque deviation and that obtained by summing both components can be defined as

$$E(t) = \Delta T_e(t) - (\,K_{syn}\,\Delta\delta(t) + K_d\,\Delta\omega(t)) \quad (23)$$

Then K_{syn} and K_d are computed to minimize the sum of the squared errors over the simulation period t_{sim} as

$$\sum_{i=1}^{N}[E_i]^2 = \sum_{i=1}^{N}\left[\Delta T_{e\,i} - \left(K_{syn}\Delta\delta_i + K_d\Delta\omega_i\right)\right]^2 \quad (24)$$

where $t_{sim} = N \times T_{samp}$, T_{samp} is the sampling period. Thus, these coefficients should satisfy

$$\frac{\partial}{\partial K_{syn}}\sum_{i=1}^{N}[E_i]^2 = 0 \text{ and } \frac{\partial}{\partial K_d}\sum_{i=1}^{N}[E_i]^2 = 0 \quad (25)$$

That yields

$$\sum_{i=1}^{N}\Delta T_{ei}\Delta\delta_i = K_{syn}\sum_{i=1}^{N}[\Delta\delta_i]^2 + K_d\sum_{i=1}^{N}[\Delta\omega_i.\Delta\delta_i] \quad (26)$$

$$\sum_{i=1}^{N}\Delta T_{e\,i}\Delta\omega_i = K_d\sum_{i=1}^{N}[\Delta\omega_i]^2 + K_{syn}\sum_{i=1}^{N}[\Delta\omega_i.\Delta\delta_i] \quad (27)$$

Solving (26) and (27), K_{syn} and K_d can be calculated.

4. IMPLEMENTATION

4.1. Real-Coded Genetic Algorithm

Due to difficulties of binary representation when dealing with continuous search space with large dimension, the proposed approach has been implemented using real-coded genetic algorithm (RCGA) [Herrera et al, 1998]. A decision variable x_i is represented by a real

Top

number within its lower limit a_i and upper limit b_i, i.e. $x_i \in [a_i,b_i]$. The RCGA crossover and mutation operators are described as follows: -

Crossover: A blend crossover operator (BLX-α) has been employed in this study. This operator starts by choosing randomly a number from the interval $[x_i - \alpha(y_i - x_i), y_i + \alpha(y_i - x_i)]$, where x_i and y_i are the i^{th} parameter values of the parent solutions and $x_i < y_i$. To ensure the balance between exploitation and exploration of the search space, $\alpha = 0.5$ is selected. This operator is depicted in Fig. 5.

Mutation: The non-uniform mutation operator has been employed in this study. In this operator, the new value $x_i^{'}$ of the parameter x_i after mutation at generation t is given as

$$x_i^{'} = \begin{cases} x_i + \Delta(t, b_i - x_i) & \text{if } \tau = 0 \\ x_i - \Delta(t, x_i - a_i) & \text{if } \tau = 1 \end{cases}, \quad (28)$$

$$\Delta(t, y) = y(1 - r^{(1-\frac{t}{g_{\max}})^{\beta}}) \quad (29)$$

where τ is a binary random number, r is a random number $r \in [0,1]$, g_{max} is the maximum number of generations, and β is a positive constant chosen arbitrarily. In this study, $\beta = 5$ was selected. This operator gives a value $x_i^{'} \in [a_i,b_i]$ such that the probability of returning a value close to x_i increases as the algorithm advances. This makes uniform search in the initial stages where t is small and very locally at the later stages.

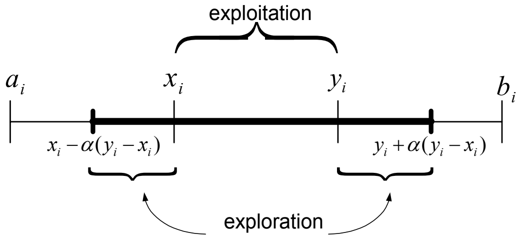

Fig. 5: Blend crossover operator (BLX-α)

4.2. RCGA Application

RCGA has been applied to search for optimal settings of the optimized parameters of the proposed control schemes. In our implementation, the crossover and mutation probabilities of 0.9 and 0.01 respectively are found to be quite satisfactory. The number of individuals in each generation is selected to be 100. In addition, the search will terminate if the best solution does not change for more than 50 generations or the number of generations reaches 500. The computational flow chart of the proposed design approach is shown in Fig. 6.

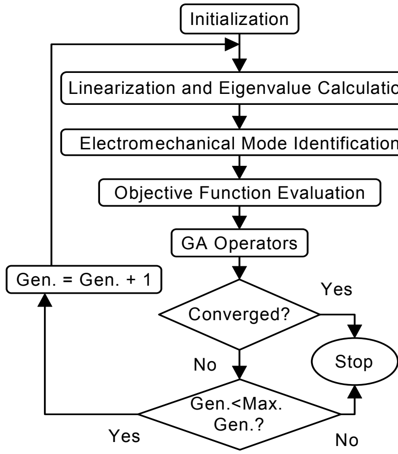

Fig. 6: Flow chart of the proposed design approach

5. RESULTS AND DISCUSSIONS

5.1. Settings of the Proposed Stabilizers

The proposed approach has been implemented on a weakly connected power system. The detailed data of the power system used in this study is given in [Yu, 1983]. The convergence rate of the objective function J with the number of generations is shown in Fig. 7 for all proposed stabilizers. The stabilizer parameters have been optimized to improve the damping ratio of the electromechanical mode eigenvalue. The final settings of the optimized parameters for the proposed stabilizers are given in Table 1. The system eigenvalues without and with the proposed stabilizers are given in Table 2 where the first row represents the electromechanical mode eigenvalues. It is clear that the electromechanical mode is unstable without control while the system stability is greatly enhanced with the proposed stabilizers.

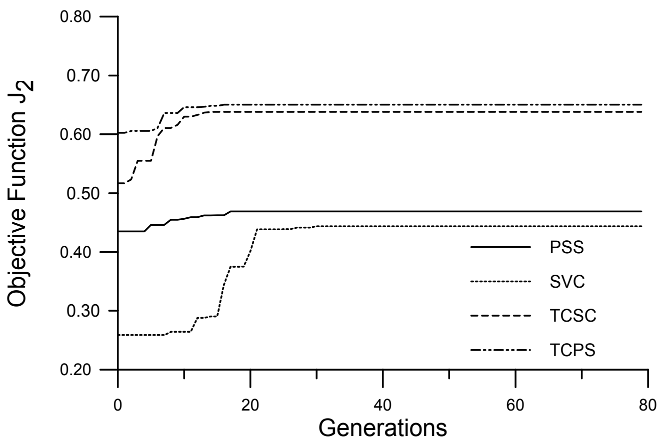

Fig. 7: Objective function convergence

Table 1: Optimal parameter settings of the proposed stabilizers

	PSS	*SVC*	*TCSC*	*TCPS*
K	17.896	98.647	99.848	99.760
T_1	0.2770	0.9587	0.0596	0.0720
T_2	0.1000	0.3000	0.1000	0.1000
T_3	----	0.0114	----	----
T_4	----	0.3000	----	----

Table 2: System eigenvalues without and with the proposed stabilizers

No Control	*PSS*	*SVC*	*TCSC*	*TCPS*
+0.30 ±*j* 4.96*	-2.71 ±*j* 5.06*	-2.33 ±*j* 4.69*	-3.28 ±*j* 3.96*	-3.05 ±*j* 3.56*
-10.39 ±*j* 3.29	-3.23 ±*j* 6.09	-2.47 ±*j* 4.98	-6.04 ±*j* 7.28	-7.08 ±*j* 8.28
------	-18.31	-20.43	-19.20	-18.03
------	-.204	-14.21	-12.36	-11.89
------	------	-2.64	-.21	-.21
------	------	-.20	------	------

5.2. Electromechanical Mode Controllability Measure

With each input signal given in (13), the minimum singular value σ_{min} has been estimated to measure the controllability of the electromechanical mode from that input. Fig. 8 shows σ_{min} with loading conditions over the range of P_e = [0.05-1.4] pu and $Q \in \{-0.4, 0.4\}$ pu. It can be seen that: -

1. The mode controllability is almost the same in case of PSS and SVC.
2. The mode is more controllable with TCSC and TCPS compared to PSS and SVC.
3. The mode controllability by TCSC changes almost linearly with the system loading.
4. The mode is most controllable by TCPS and TCSC at light loading and heavy loading respectively.
5. As Q increases, the mode controllability via TCSC becomes dominant at lower loading levels.

5.3. Damping Torque Coefficient

In order to evaluate the effectiveness of the proposed stabilizers, the damping torque coefficient was estimated with each stabilizer. Fig. 9 shows K_d vs. the loading variations. It can be concluded that: -

1. The damping of the TCPS is almost independent of loading variations.
2. The damping of the TCSC increases linearly with P_e.
3. The SVC provides negative damping al low loading conditions. This becomes more evident with positive Q as shown in Fig. 9-(c).
4. PSS outperforms the SVC for low loading levels.

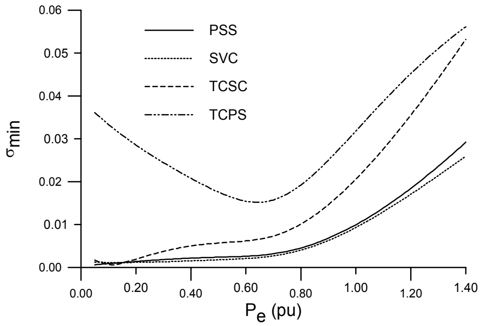

(a)

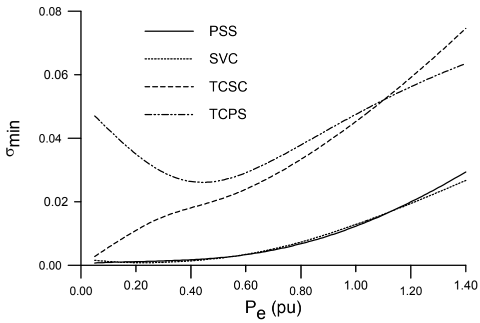

(b)

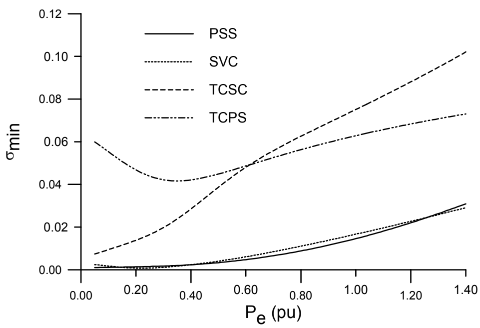

(c)

Fig. 8: Minimum singular value with loading variations.
(a) Q = -0.4 pu, (b) Q = 0.0 pu, (c) Q = 0.4 pu

Top

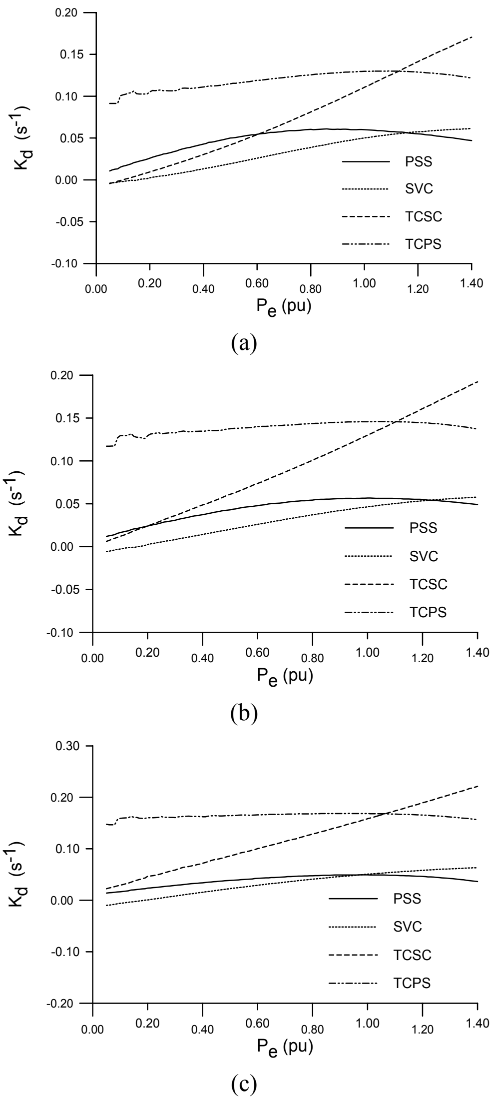

Fig. 9: Damping coefficient with the loading variations.
(a) Q = -0.4 pu, (b) Q = 0.0 pu, (c) Q = 0.4 pu

5.4. Nonlinear Simulation Results

For completeness and verification, all the proposed stabilizers were tested under different disturbances and loading conditions. Fig. 10 shows the system response with 6-cycle fault disturbance at the nominal loading condition. It can be seen that the TCPS and TCSC provide the best damping characteristics and enhance greatly the first swing stability. This is found to be consistent with the damping torque coefficient results shown in Fig. 9-(b). On the other

Top

hand, the terminal voltage has great variations with the PSS. The results with a 3-cycle fault disturbance at a heavy loading condition are shown in Fig. 11. It is clear that the TCSC provides the greatest damping characteristics at this loading. This confirms the findings of Fig. 9-(c).

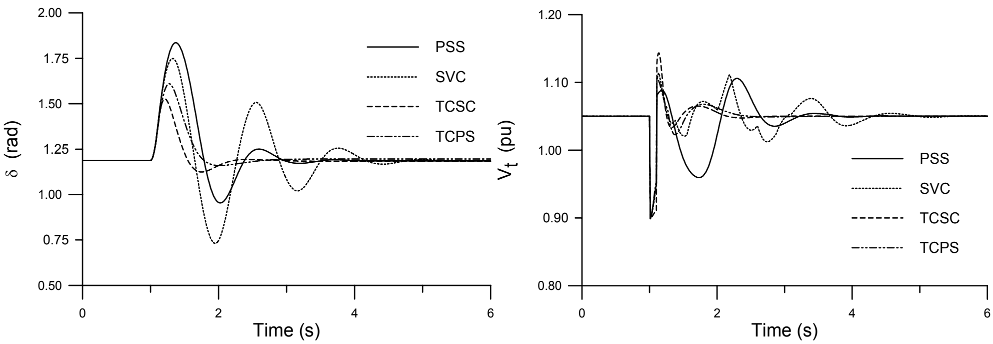

(a) (b)

Fig. 10: System response for 6-cycle fault disturbance with loading (P=1.0 pu, Q=0.015 pu)
(a) Rotor angle response (b) Terminal voltage response

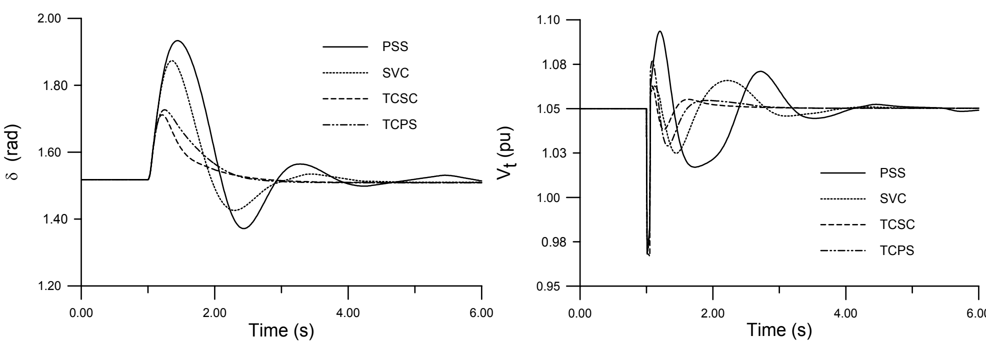

(a) (b)

Fig. 11: System response for 6-cycle fault disturbance with loading (P=1.1 pu, Q=0.4 pu)
(a) Rotor angle response (b) Terminal voltage response

6. CONCLUSION

In this study, the power system stability enhancement via PSS and FACTS-based stabilizers is presented and discussed. For the proposed stabilizer design problem, an eigenvalue-based objective function to increase the system damping was developed. Then, the real-coded genetic algorithm was implemented to search for the optimal stabilizer parameters. In addition, a controllability measure for the poorly damped electromechanical modes using a singular value decomposition approach is proposed to assess the effectiveness of the proposed stabilizers. The damping characteristics of the proposed schemes were also evaluated in terms of the damping torque coefficient. The proposed stabilizers have been tested on a weakly connected power system with different loading conditions. The nonlinear simulation results show the effectiveness and robustness of the proposed stabilizers to enhance the system stability.

ACKNOWLEDGEMENT

The authors acknowledge the support of King Fahd University of Petroleum & Minerals via funded Project # FT/2000-25.

REFERENCES

1. Chang, J. and Chow, J., 1997, "Time Optimal Series Capacitor Control for Damping Inter-Area Modes in Interconnected Power Systems," *IEEE Trans. PWRS,* Vol. 12, No. 1, pp. 215-221.
2. Chen, X., Pahalawaththa, N., Annakkage, U., and Kumble, C., 1995, "Controlled Series Compensation for Improving the Stability of Multimachine Power Systems," *IEE Proc*., Pt. C, Vol. 142, pp. 361-6.
3. Edris, A., 1991, "Enhancement of First-Swing Stability Using a High-Speed Phase Shifter," *IEEE Trans. PWRS,* Vol. 6, No. 3, pp. 1113-1118.
4. Failat, E. A., Bettayyeb, M., Al-Duwaish, H., Abido, M. A., and Mantawy, A., 1996, “A neural network based approach for on-line dynamic stability assessment using synchronizing and damping torque coefficients,” *Electrical Power Systems Research,* Vol. 39, No. 2, pp. 103-110.
5. Hamdan, A. M. A., 1999, “An Investigation of the Significance of Singular Value Decomposition in Power System Dynamics,” Int. Journal of Electrical Power and Energy Systems, Vol. 21, pp. 417-424.
6. Hammad, A. E., 1986, "Analysis of Power System Stability Enhancement by Static VAR Compensators," *IEEE Trans. PWRS,* Vol. 1, No. 4, pp. 222-227.
7. Herrera, F., Lozano, M., and Verdegay, J. L., 1998, “Tackling Real-Coded genetic Algorithms: operators and Tools for Behavioral Analysis,” Artificial Intelligence Review, Vol. 12, No. 4, pp. 265-319.
8. Hiyama, T., Mishiro, M., Kihara, H., and Ortmeyer, T. H., 1995, “Coordinated Fuzzy Logic Control for Series Capacitor Modules and PSS to Enhance Stability of Power System,” *IEEE Trans. PWRD,* Vol. 10, No. 2, pp. 1098-1104.
9. Hsu, Y. Y. and Chen, C. L., 1987, “Identification of optimum location for stabilizer applications using participation factors,” *IEE Proc*., Pt. C, Vol. 134, No. 3, pp. 238-244.

10. Jiang, F., Choi, S. S., and Shrestha, G., 1997, "Power System Stability Enhancement Using Static Phase Shifter," *IEEE Trans. PWRS,* Vol. 12, pp. 207-214.
11. Mahran, A. R., Hogg, B. W., and El-Sayed, M. L., 1992, "Coordinated Control of Synchronous Generator Excitation and Static VAR Compensator," *IEEE Trans. Energy Conversion,* Vol. 7, pp. 615-622.
12. Noroozian, M. and Anderson, G., 1994, "Damping of Power System Oscillations by Use of Controllable Components," *IEEE Trans. PWRD,* Vol. 9, No. 4, pp. 2046-2054.
13. Padiyar, K. R. and Varma, R. K., 1991, "Damping Torque Analysis of Static VAR System Oscillations," *IEEE Trans. PWRS,* Vol. 6, No. 2, pp. 458-465.
14. Rahim, A. and Nassimi, S., 1996, "Synchronous Generator Damping Enhancement Through Coordinated control of Exciter and SVC," IEE Proc. Gener. Transm. Distrib., Vol. 143, No. 2, pp. 211-218.
15. Sauer, P. W. and Pai, M. A., 1998, Power system Dynamics and Stability, Prentice Hall.
16. Wang, H. F. and Swift, F. J., 1998, "A Unified Model for the Analysis of FACTS Devices in Damping Power System Oscillations Part I: Single-machine Infinite-bus Power Systems," *IEE Proc. Genet. Transm. Distrib.*, Vol. 145, No. 2, pp. 111-116.
17. Yu, Y. N., 1983, Electric Power System Dynamics, Academic Press, USA.

Top